International Journal of Civil Engineering

Geotechnical Engineering

A continuum fluid-particle coupled piping model based on solute transport

Y. L. Luo*

Received: May 2011, Revised: June 2012, Accepted: November 2012

Abstract

The occurrence of piping failures in earth structures demonstrates the urgency and importance of studying piping. With this intention, a new piping model was developed in the framework of continuum mixture theory. Assuming that porous media are comprised of solid skeleton phase, fluid phase and fluidized fine particles phase, the fluidized fine particles phase is considered to be a special solute migrating with the fluid phase. The three phases interact while being constrained by the mass conservation equations of the three phases, and a sink term was introduced into the mass conservation equation of the solid skeleton phase to describe the erosion of fluidized fine particles, then a new continuum fluid-particle coupled piping model was established and validated. The validation indicates that the proposed model can predict the piping development of complicated structures under complex boundary and flow conditions, and reflect the dynamic changes of porosity, permeability and pore pressure in the evolution of piping.

Keywords: *Piping, Fluid-particle interaction, Solute transport, Continuum mixture theory.*

1. Introduction

Piping, defined as the erosion and migration of fine particles under seepage, is the most serious menace to the safety of dam. In Foster et al.'s survey of 11192 dams, around 46% of dams' failures were related to piping [1]. It also has been demonstrated that the potential for loss of life in the event of a dam failure is very dependent on the warning time, U.S. Bureau of Reclamation (USBR) suggests that an advance warning of failure of as little as 60 minutes can have a significant impact on reducing the number of lives lost [2, 3]. So predicting the evolution of piping or giving an advance warning before piping failure are very meaningful and urgent, but improvements in this area are hindered by the complexity of piping mechanism and the difficulties of piping detection.

From a mechanics standpoint, the development of a numerical piping model is a challenging task, it involves capturing the whole range of material response from solid-like to fluid-like behavior. During the last decades, several numerical models have been developed. Fell et al. [4] defined a logical framework to give an approximate estimate of the time for piping based on the characteristics of a dam and its foundation. Goodarzi et al. [5] proposed a probability model estimating the probability of piping failure using an event tree method. Sterpi [6] developed a continuum model based on the mass conservation of eroded fine particles and a suitable law of erosion. Cividini and Gioda [7] proposed a similar finite-element model by combining the mass continuity equation of transported particles and the erosion law used in [6]. But the influences of erosion on the hydraulic conductivity and seepage velocity are not considered in the two continuum models proposed by Sterpi [6] and Cividini et al. [7]. Bonelli and Lachouette et al. [8, 9, 10] developed a piping model from the diphasic flow equations with diffusion and the jump equations with erosion, and simulated the hole erosion test. El Shamy et al. [11, 12] established a multi-scale model to simulate flood-induced piping under river levees. Maeda and Sakai et al. [13, 14] developed a continuum-discrete model by 'Smoothing Particles Hydrodynamics (SPH)'. However, the multi-scale or continuum-discrete model is limited since it requires considerable computer power, a precise description of contact behavior between granular particles, and a rigorous incorporation with fluid.

* *Corresponding Author: lyl8766@hhu.edu.cn*
College of Water Conservancy and Hydropower Engineering, Hohai University, Nanjing 210098, China

Based on a comprehensive assessment on the existing models, the continuum model is still a powerful alternative modeling framework, so this paper developed a new continuum piping model based on solute transport. Contrasting with the existing numerical models, the main improvements of the new model are as follows: (a) Assuming that porous media are comprised of solid skeleton phase, fluid phase and fluidized fine particles phase, the fluidized fine particles phase is considered to be a special solute transporting with the fluid phase. (b) The fluid-particle interaction is considered by combining the three phase's mass conservation equations with a sink term describing the erosion of fine particles, and the influences of eroded fine particles on the porosity and pore pressure are considered in the evolution of piping. The new model can predict the piping development of complicated structures under complex boundary and flow conditions, and reflect the dynamic changes of porosity, permeability and pore pressure induced by the erosion and migration of fine particles.

2. A New Continuum Piping Model

2.1 Basic assumptions and definitions

Basic assumptions: (1) Saturated porous media are modeled as a three-phase system consisting of solid skeleton (*ss*), fluid (*f*) and fluidized fine particles (*ff*). The fluidized fine particles phase is considered to be a special solute migrating with the fluid phase. (2) The pores are completely filled with fluid and fluidized fine particles. (3) The solid skeleton phase is rigid, and the fluid phase is incompressible. (4) The fluid phase and fluidized fine particles phase always share the same velocity.

Basic definitions: (1) Volume fraction of α phase, $n^{\alpha}=dV^{\alpha}/dV$ where α phase represents solid skeleton phase, fluidized fine particles phase and fluid phase, dV^{α} is the volume of α phase, dV is the representative elementary volume (REV). (2) Partial density of α phase, $\rho^{\alpha}=dm^{\alpha}/dV$, where dm^{α} is the mass of α phase. (3) Real density of α phase, $\rho^{\alpha'}=dm^{\alpha}/dV^{\alpha}=\rho^{\alpha}/n^{\alpha}$, for the solid skeleton phase and the fluidized fine particles phase, $\rho^{ss'}=\rho^{ff'}=\rho^{\alpha}=\rho^{s'}$, $\rho^{s'}$is the real density of soil particle, and $\rho^{f'}$ is the real density of fluid. (4) Porosity, $\phi=dV_v/dV=n^{f}+n^{ff}$, where dV_v is the volume of pores. (5) Volume concentration of fluidized particles, $c=dV^{ff}/dV_v=n^{ff}/(n^{f}+n^{ff})$.

2.2 Governing Differential Equations

For multi-phase flow system, the mass conservation equation can be expressed [15]:

$$\frac{\partial \rho^{\alpha}}{\partial t}+div(\rho^{\alpha}v^{\alpha'})=\dot{m}^{\alpha} \tag{1}$$

where $V^{\alpha'}$ is the real velocity of α phase. The first term on the left in Equation (1) denotes the partial density change rate of α phase, and the second term is the net accumulation mass rate of α phase. The right term is a mass generation term, which indicates the mass generation rate of α phase. Therefore, the mass conservation equations of the three phases are:

Solid skeleton phase: $$\frac{\partial \phi}{\partial t}=\frac{\dot{m}^{ff}}{\rho^{s'}} \tag{2}$$

Fluidized fine particles phase: $$\frac{\partial c\phi}{\partial t}+v_x\frac{\partial c}{\partial x}+v_y\frac{\partial c}{\partial y}=\frac{\partial \phi}{\partial t} \tag{3}$$

Fluid phase: $$\frac{\partial v_x}{\partial x}+\frac{\partial v_y}{\partial y}=0 \tag{4}$$

where v_x , v_x are seepage velocities in the direction of x and y, respectively, t denotes time. Equations (2)~(4) contain five basic unknowns ϕ, c, v_x, v_y, $\dot{m}^{ff}$, a constitutive equation for $\dot{m}^{ff}$ is needed for solving this problem, and here the equation used in [16] was adopted:

$$\dot{m}^{ff}=\dot{m}_{er}-\dot{m}_{dep}=\rho^{s'}\lambda(1-\phi)c\sqrt{v_x^2+v_x^2}-\rho^{s'}\lambda(1-\phi)\frac{c^2}{c_{cr}}\sqrt{v_x^2+v_x^2} \tag{5}$$

Equation (5) is related to the filtration of non-colloidal solid particles in porous media. $\dot{m}^{ff}$ is comprised of two terms $\dot{m}_{er}$ and $\dot{m}_{dep}$, where $\dot{m}_{er}$ is the rate of eroded mass, $\dot{m}_{er}=\rho^{s'}\lambda(1-\phi)c\sqrt{v_x^2+v_x^2}$, and $\dot{m}_{dep}$ is the deposited mass rate, $\dot{m}_{dep}=\rho^{s'}\lambda(1-\phi)\frac{c^2}{c_{cr}}\sqrt{v_x^2+v_x^2}$, where c_{cr} is a critical value of c, and c_{cr}=0.3 was adopted in this paper. λ has the dimension of inverse length, it is related to the spatial frequency of the potential erosion starter points and can be determined experimentally.

The relationship between hydraulic conductivity and seepage velocity can be expressed by Darcy Law:

$$v_x=-\frac{k'}{\bar{\rho}g}\frac{\partial p}{\partial x},\quad v_y=-\frac{k'}{\bar{\rho}g}\frac{\partial p}{\partial y} \tag{6}$$

$$k'=\frac{k\bar{\rho}g}{\mu} \tag{7}$$

where k' is the hydraulic conductivity of porous media, p is the pore pressure, $\bar{\rho}$ is the density of fluid and fluidized fine particles mixture, $\bar{\rho}=c\rho^{s'}+(1-c)\rho^{f'}$. μ is the coefficient of dynamic viscosity of the mixture, $\mu=\eta_k\bar{\rho}$, η_k is the coefficient of kinematic viscosity of the mixture, k is the intrinsic permeability of porous media. In addition, the intrinsic permeability can be expressed by the porosity using Kozeny-Carman formula:

$$k=k_0\frac{\phi^3}{(1-\phi)^2} \tag{8}$$

where k_0 indicates the initial intrinsic permeability of porous media. Substituted Equations (5)~(8) into Equations (2)~(4), the governing differential equations of the new continuum piping model can be expressed as follows:

$$\frac{\partial c\phi}{\partial t}-\frac{k_0}{\eta_k\bar{\rho}}\frac{\phi^3}{(1-\phi)^2}\frac{\partial p}{\partial x}\frac{\partial c}{\partial x}-\frac{k_0}{\eta_k\bar{\rho}}\frac{\phi^3}{(1-\phi)^2}\frac{\partial p}{\partial y}\frac{\partial c}{\partial y}-\frac{k_0}{\eta_k\bar{\rho}}\frac{\phi^3}{(1-\phi)^2}\bar{\rho}g\frac{\partial c}{\partial y}=\frac{\partial \phi}{\partial t} \tag{9}$$

$$\frac{\partial \phi}{\partial t}=\lambda(1-\phi)(c-\frac{c^2}{c_{cr}})\frac{k_0}{\eta_k\bar{\rho}}\frac{\phi^3}{(1-\phi)^2}\sqrt{(\frac{\partial p}{\partial x})^2+(\frac{\partial p}{\partial y}+\bar{\rho}g)^2} \tag{10}$$

$$\frac{\partial^2 p}{\partial x^2}+\frac{\partial^2 p}{\partial y^2}+\frac{3-\phi}{\phi(1-\phi)}(\frac{\partial p}{\partial x}\frac{\partial \phi}{\partial x}+\frac{\partial p}{\partial y}\frac{\partial \phi}{\partial y}+\bar{\rho}g\frac{\partial \phi}{\partial y})-\frac{\rho^{s'}-\rho^{f'}}{\bar{\rho}}(\frac{\partial p}{\partial x}\frac{\partial c}{\partial x}+\frac{\partial p}{\partial y}\frac{\partial c}{\partial y}+\bar{\rho}g\frac{\partial c}{\partial y})=0 \tag{11}$$

The basic unknowns in Equations (9)~(11) are only ϕ, c and p. The Galerkin method and implicit difference method were

adopted to discretize space and time in Equations (9)~(11), respectively, and then the Newton-Raphson iterative method was applied to solve the discrete linear equations.

2.3 Global Matrix Storage and Solution Strategy

Due to the existence of pure convection terms ($v_x \partial c/\partial x$ and $v_y \partial c/\partial y$) in Equation (9), the global matrix of the new model is extremely ill-conditioned (the maximum condition number is up to 10^{14}.) and non-symmetric. In addition, the main diagonal entries are not absolutely dominant (some main diagonal entries are negative.). How to storage and solve such complicated global matrix is a very challenging task.

2.3.1 Global Matrix Storage Strategy

The Compressed Sparse Row method (CSR) [17] was adopted to store the nonsymmetric global matrix in this paper. On the one hand, the CSR method can save a lot of storage space; on the other hand, it is very suitable for the successive matrix operations.

2.3.2 Global Matrix Solution Strategy

The solution of the global matrix is also a tough job, because the traditional iterative methods can do nothing about it owing to the nondominant main diagonals. Fortunately the Stable Bi-conjugate Gradient method (BICGSTAB(1)) is an efficient algorithm in Krylov subspace method [18], it provides an effective tool for solving nonsymmetric, ill-conditioned matrix, but the convergence speed is closely related to the condition number of the matrix, so a good preconditioner is needed to reduce the condition number in advance.

A preconditioner is any form of implicit or explicit modification of an original linear system. On the basis of comparing the performance and speed of various preconditioners, the zero fill-in incomplete LU factorization (ILU(0)) was adopted [17], and the algorithm of ILU(0)-BICGSTAB(1) can be seen in [19]. According to the above description, a nonlinear finite element program called SEP was developed, and it was validated in the next section.

3. Validation

3.1 Example 1

Stavropoulou et al. [20] presented a sand production numerical model in petroleum engineering. The sand production can leads to various problems such as the accumulation of sand in the wellbore and the formation of unstable cavities in the geological formation, it is similar to the backwards erosion piping. In the backwards erosion piping, fine particles are progressively dislodged from the soil matrix through tractive forces produced by intergranular seepage water. The erosive forces are greatest where flow concentrates at an exit point and once soil particles are removed by erosion the magnitude of the erosive forces increases due to the increased concentration of flow [21].

Fig. 1 shows the finite element model. The wellbore radius r_0=0.1m, outer boundary radius r_a=5.0m. Initial conditions: porosity $\phi(r, 0)$=0.25, transport concentration $c(r, 0)$=0.001, pore pressures in the whole region were obtained from the initial steady seepage calculation. Boundary conditions: transport concentration on the outer boundary $c(r_a, t)$=0.001, wellbore fluid pressure $p(r_0, t)$=5.0 *MPa*, pore pressure on the outer boundary $p(r_a, t)$=8.0 *MPa*. Computing time is 8000 *sec*. Table 1 shows the basic mechanical parameters. Fig. 2 demonstrates the time variation of porosity and transport concentration at free surface ($r=r_0$), Fig. 3 depicts the spatial profiles of porosity and pore pressure at t=6800 *sec*, Fig. 4 shows the field variables distributions at t=3000 *sec* and 8000 *sec*.

It can be seen from Fig. 2 that the results gained here are consistent with the literature [20]. The porosity and transport

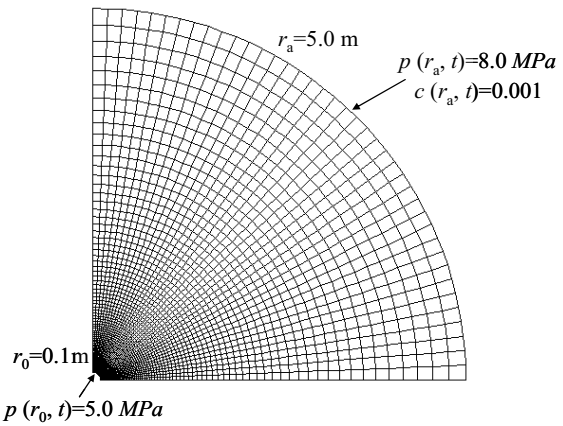

Fig. 1 Finite element mesh for the Example 1

Table 1 Material parameters of Example 1

k_0(m^2)	η_k(m^2/s)	$\rho^{f'}$(kg/m^3)	$\rho^{s'}$(kg/m^3)	λ(m^{-1})
1.3×10^{-11}	5.0×10^{-6}	840.0	2650.0	5.0

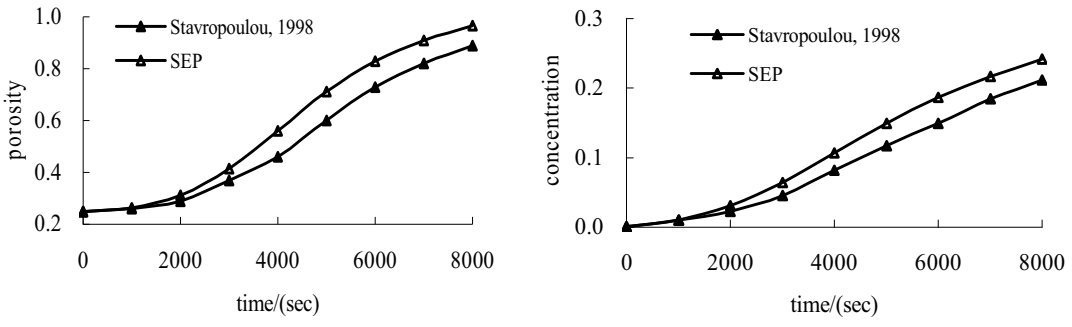

Fig. 2 Time variation of porosity and transport concentration at free surface

concentration at free surface increase slowly when time is less than 2000 *sec*, while the both increase rapidly from 0.27, 0.01 to 0.81 and 0.18 respectively at 2000 *sec*<*t*<7000 *sec*, and then the both increase slowly again when time is larger than 7000 *sec*, the porosity tends to 1.0, and the transport concentration eventually converges to the critical value c_{cr}=0.3.

Fig. 3 shows that the results gained here are consistent with the literature [20] at *t*=6800 *sec*. The porosity near the free surface changes sharply, it indicates that the erosion near the free surface is the most serious in the whole region, which in

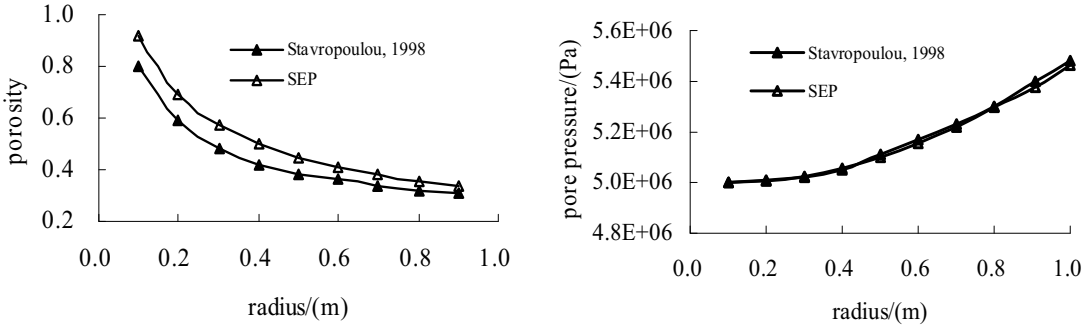

Fig. 3 Spatial profiles of porosity and pore pressure at t=6800 *sec*

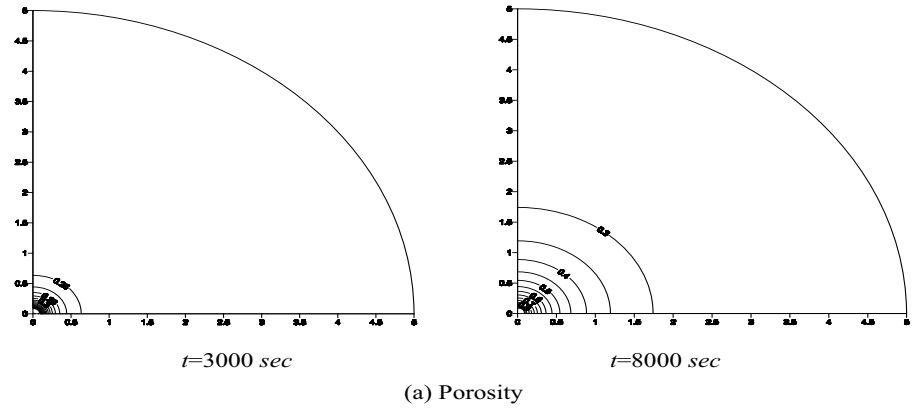

(a) Porosity

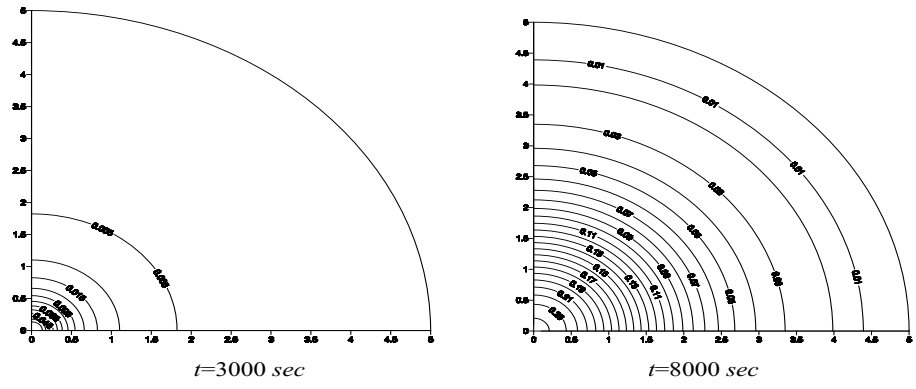

(b) Transport concentration

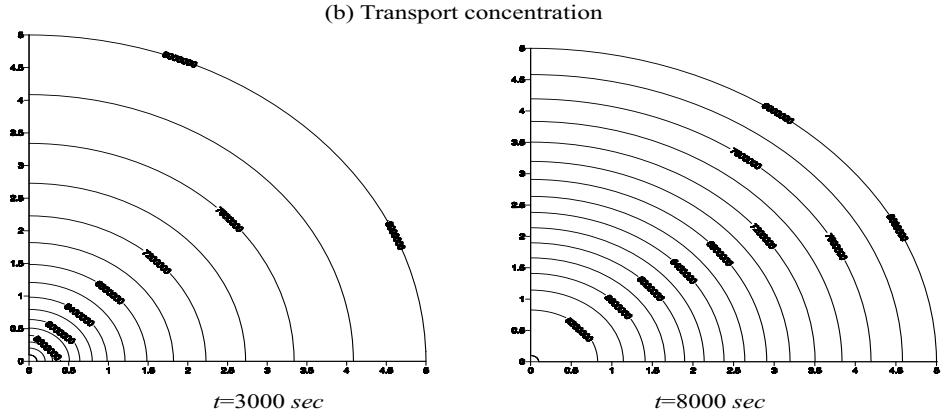

(c) Pore pressure (unit: *Pa*)

Fig. 4 Contours of field variables at t=3000 *sec* and 8000 *sec*

turn results in the lowest pressure gradient near the free surface.

Fig. 4 demonstrates that only the porosity and concentration increase rapidly near the free surface, and yet the both far away from the free surface are in the vicinity of the initial values. The change of pore pressure is different from the porosity and concentration, only the pore pressure gradient near the free surface changes sharply at the beginning, and then it becomes linear distribution gradually.

3.2 Example 2

The evolution of piping in sheet-pile and sand foundation was presented in Example 2, which is called "internal erosion", it is similar to the backwards erosion piping. However, it is due to flow along pre-existing openings such as cracks in cohesive material or voids along a soil-structure contact, it is initiated by erosive forces of water along the soil-structure contact [21].

Fig. 5 demonstrates the geometry and finite element model. Table 2 shows the material parameters. Initial conditions: the initial porosity and transport concentration are 0.25 and 0.001 respectively, the initial pore pressures in the whole region were obtained from the initial saturated steady seepage analysis. Boundary conditions: the pore pressures on the upstream and downstream are 0.1 *MPa* and 0 *MPa*, respectively. Computing time is 10000 *sec*, Fig. 6~7 show the time variation of porosity and transport concentration. Fig. 8 depicts the equip-potential lines at t=10000 *sec*.

Fig. 6 indicates that the porosity at the bottom of sheet-pile is always the largest. This is because the hydraulic gradient and seepage velocity at the bottom of sheet-pile are the largest, and the erosion in this area is also the most serious in the whole region.

Fig. 7 shows that the change of transport concentration is more complicated than that of porosity. The transport concentration at the bottom of sheet-pile is the largest at the

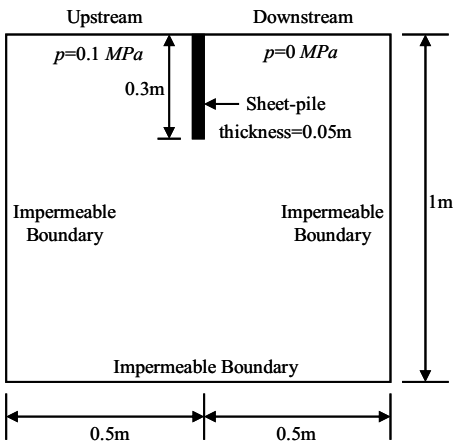

Fig. 5 Sheet-pile model for the Example 2

Table 2 Material parameters of Example 2

k_0(m^2)	η_k(m^2/s)	$\rho^{f'}$ (kg/m^3)	$\rho^{s'}$ (kg/m^3)	λ(m^{-1})
1.3×10^{-11}	5.0×10^{-6}	840.0	2650.0	5.0

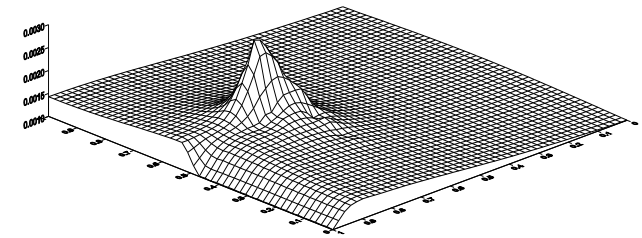

(a) t=1000 *sec*

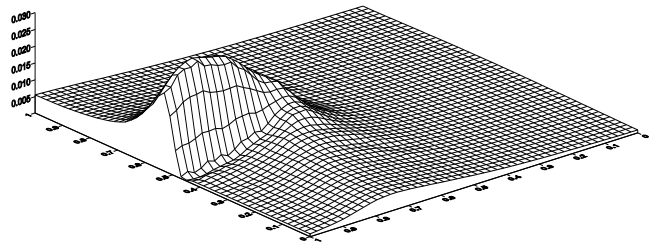

(b) t=5000 *sec*

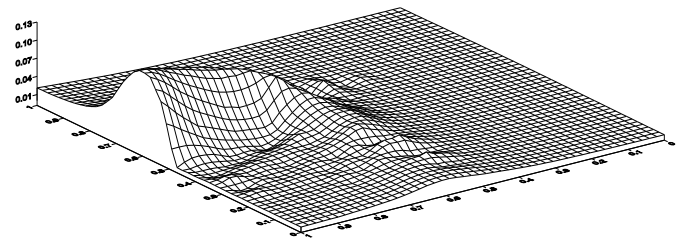

(c) t=10000 *sec*

Fig. 7 Time variation of transport concentration

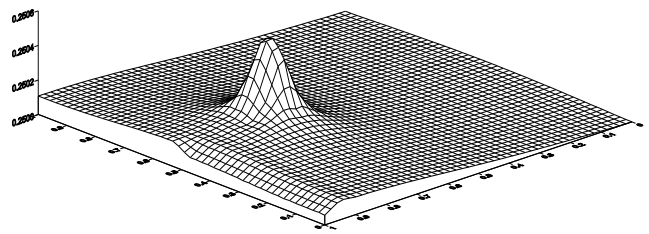

(a) t=1000 *sec*

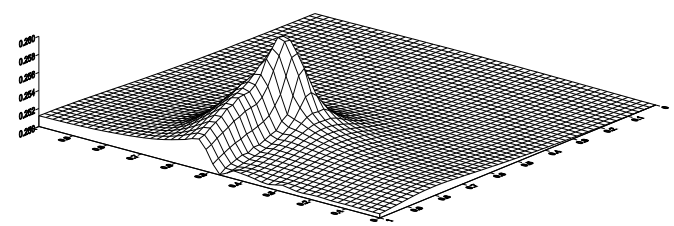

(b) t=5000 *sec*

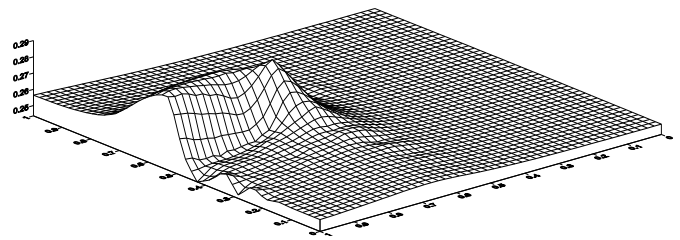

(c) t =10000 *sec*

Fig. 6 Time variation of porosity

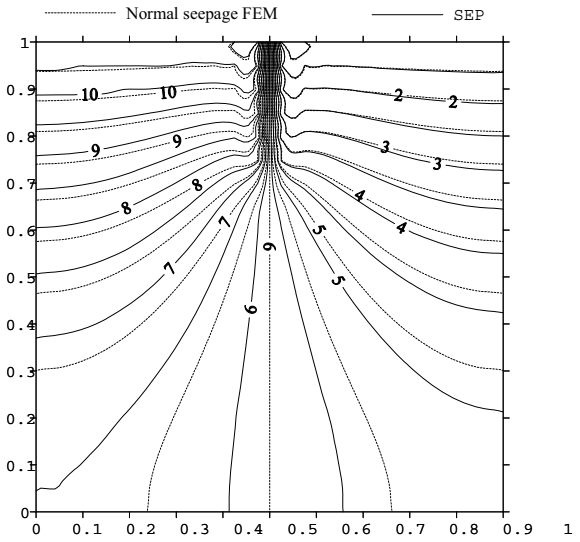

Fig. 8 Comparison of the equip-potential lines at t=10000 *sec* (unit: m)

beginning, and then that near the downstream becomes the largest gradually due to the collection of eroded fine particles.

Fig. 8 demonstrates that the equip-potential lines calculated by SEP are quite different from that calculated by normal seepage FEM, especially at the bottom of sheet-pile. The reason may be that the nonuniform change of permeability due to the migration of eroded fine particles leads to the redistribution of pore pressure in the whole region, at the same time the change of the pore pressure influences the migration of fine particles and the evolution of piping channel. In a word, the fluid-particle interaction is very significant in the evolution of piping, which has been embodied in the new continuum piping model, so it is concluded that the new model proposed here is more advantageous than the normal seepage FEM.

4. Conclusions and Perspectives

In the framework of continuum mixture theory, a new continuum fluid-particle coupled piping model was proposed based on solute transport. The new model considers the fluid-particle interaction in the evolution of piping, it can predict the piping development of complicated structures under complex boundary and flow conditions, reflect the dynamic changes of porosity, permeability and pore pressure induced by the eroded fine particles, depict the unsteady, progressive failure characteristics of piping. These improvements make up for the shortages of the existing numerical models, which would provide a new dimension to the design of earth structures.

However, some improvements on the new model still need to be done in the future: (1) The new model tends to exhibit numerical oscillations in some cases, so improvement on the numerical stability should be done urgently. (2) The new model in this paper can not be used to predict the fractured rock mass failure due to piping, how to establish a suitable piping model for the fractured rock mass is yet to be further studied. (3) The current study does not adequately consider the mechanical coupling effect, for example, the erosion and migration of fine particles will eventually change the shear strength and stress status of porous media, and induce sequent deformation, even collapse. Now the author is designing a triaxial piping test apparatus, it is hoped that a new seepage-erosion-stress coupling piping mechanism and a more comprehensive numerical model will be proposed in the near future.

Acknowledgments: The supports of the Natural Science Foundation of China under project No.51009053 is gratefully acknowledged.

References

[1] Foster, M., Fell, R. and Spannagle, M.: 2000, Statistics of Embankment Dam Failures and Accidents, Canadian Geotechnical Journal, 37(5), 1000-1024.

[2] U.S. Bureau of Reclamation (USBR): 1999, A Procedure for Estimating Loss of Life Caused by Dam Failure, Publication No. DSO-99-06, U.S. Bureau of Reclamation, Denver.

[3] Fell, R., Wan, C.F. and Foster, M.A.: 2004, Methods for Estimating the Probability of Failure of Embankment Dams by Internal Erosion and Piping-Piping Through the Embankment, UNICIV Report No R-428, University of New South Wales, Sydeney.

[4] Fell, R., Wan, C.F., Cyganiewicz, J., et al.: 2003, Time for Development of Internal Erosion and Piping in Embankment Dams, Journal of Geotechnical and Geoenvironmental Engineering, 129(4), 307-314.

[5] Goodarzi, E., Shui, L.T., Ziaei, M., et al.: 2010, Estimating Probability of Failure due to Internal Erosion with Event Tree Analysis, Electronic Journal of Geotechnical Engineering, 15(10), 935-948.

[6] Sterpi, D.: 2003, Effects of the Erosion and Transport of Fine Particles due to Seepage Flow, International Journal of Geomechanics, 3(1), 111-122.

[7] Cividini, A., Gioda, G.: 2004, Finite Element Approach to the Erosion and Transport of Fine Particles in Granular Soils, International Journal of Geomechanics, 4(3), 191-198.

[8] Bonelli, S., Brivois, O., Borghi, R., et al.: 2006, On the Modeling of Piping Erosion, Comptes Rendus Mécanique, 334(8-9), 556-559.

[9] Bonelli, S., Brivois, O.: 2008, The Scaling Law in the Hole Erosion Test with A Constant Pressure Drop. International Journal for Numerical and Analytical Methods in Geomechanics, 32(13), 1573-1595.

[10] Lachouette, D., Golay, F. and Bonelli, S.: 2008, One-dimensional Modeling of Piping Flow Erosion. Comptes Rendus Mécanique, 336(9), 731-736.

[11] El Shamy, U., Zeghal, M.: 2005, Coupled Continuum-Discrete Model for Saturated Granular Soils, Journal of Engineering Mechanics, 131(4), 413-426.

[12] El Shamy, U., Aydin, F.: 2008, Multiscale Modeling of Flood-Induced Piping in River Levees, Journal of Geotechnical and Geoenvironmental Engineering, 134(9), 1385-1398.

[13] Maeda, K., Sakai, H. and Sakai, M.: 2006, Development of Seepage Failure Analysis Method of Ground with Smoothed Particle Hydrodynamics, Structural Engineering/Earthquake Engineering, 23(2), 307-319.

[14] Sakai, H., Maeda, K.: 2009, Seepage Failure and Erosion Mechanism of Granular Material With Evolution of Air Bubbles Using SPH, Proceedings of the 6th International Conference on Micromechanics of Granular Media, Golden, Colorado, 1001-1004.

[15] Bear, J.: 1972, Dynamics of Fluids in Porous Media, New York: American Elsevier.
[16] Vardoulakis, I., Stavropoulou, M. and Papanastasiou, P.: 1996, Hydro-Mechanical Aspects of the Sand Production Problem, Transport in Porous Media, 22(2), 225-244.
[17] Yousef, S.: 2000, Iterative Methods for Sparse Linear Systems, Philadelphia: Society for Industrial and Applied Mathematics.
[18] Vogel, J. A.: 2007, Flexible BICG and Flexible Bi-CGSTAB for Nonsymmetric Linear System, Applied Mathematics and Computation, 188(1), 226-233.
[19] Smith, I.M., Griffiths, D.V.: 2004, Programming the Finite Element Method. 4th ed, New York: John Wiley & Sons.
[20] Stavropoulou, M., Papanastasiou, P. and Vardoulakis, I.: 1998, Coupled Wellbore Erosion and Stability Analysis, International Journal for Numerical and Analytical Methods in Geomechanics, 22(9), 749-769.
[21] Richards, K.S., Reddy, K.R.: 2007, Critical Appraisal of Piping Phenomena in Earth Dams, Bulletin of Engineering Geology and the Environment, 66(4), 381-402.\

Notation

α	Solid skeleton (*ss*), fluid (*f*) and fluidized fine particles (*ff*)
n^{α}	Volume fraction of α phase
ρ^{α}	Partial density of α phase (kg/m^3)
$\rho^{\alpha\prime}$	Real density of α phase (kg/m^3)
$\rho^{s\prime}$	Real density of soil particle (kg/m^3)
$\rho^{f\prime}$	Real density of fluid (kg/m^3)
ϕ	Porosity
c	Volume concentration of fluidized particles
dV^{α}	Volume of α phase (m^3)
dV	Representative elementary volume (m^3)
dV_v	Pore volume (m^3)
dm^{α}	Mass of α phase (kg)
t	Time (sec)
$v^{\alpha\prime}$	Real velocity of α phase (m/s)
$\dot{m}^{\alpha}$	Mass generation term (kg/sec)
v_x, v_y	Seepage velocities in the direction of x and y (m/s)
$\dot{m}_{er}$	Rate of eroded mass (kg/sec)
$\dot{m}_{dep}$	Deposited mass rate (kg/sec)
c_{cr}	Critical value of c
λ	Spatial frequency of erosion starter points (m^{-1})
k'	Hydraulic conductivity (m/s)
p	Pore pressure (Pa)
$\bar{\rho}$	Density of fluid and fluidized fine particles mixture (kg/m^3)
μ	Coefficient of dynamic viscosity of the mixture (Pa.s)
η_k	Coefficient of kinematic viscosity of the mixture (m^2/s)
k_0	Initial intrinsic permeability (m^2)